RSC Advances

PAPER

View Article Online
View Journal | View Issue

A rhodamine B-based "turn-on" fluorescent sensor for detecting Cu^{2+} and sulfur anions in aqueous media†

Cite this: *RSC Adv.*, 2014, **4**, 5718

Dan Guo,[ab] Zhengping Dong,[a] Chao Luo,[a] Wenyan Zan,[a] Shiqiang Yan*[a] and Xiaojun Yao[a]

Received 18th October 2013
Accepted 11th December 2013

DOI: 10.1039/c3ra45931d

www.rsc.org/advances

A novel selective fluorescent chemosensor **L** based on rhodamine B derivative has been designed and synthesized to optically detect Cu^{2+} and S^{2-} in aqueous buffer solution. The fluorescence of **L** was excited by Cu^{2+} with a 1 : 1 binding ratio, and could be used as a "turn-on" type sensor. Otherwise, the emission band would undergo a slight red-shift. Once binding with Cu^{2+}, the copper complex can exhibit high selectivity for S^{2-}. Upon addition of Cu^{2+}, the color of the chemosensor **L** changes from colorless to pink. Additionally, the resulting pink solution changes to colorless immediately upon the addition of S^{2-}. However, no phenomenon change could be observed in the presence of other anions. Conclusively, the color changes suggest that sensor **L** could serve as a "naked-eye" sensor for Cu^{2+} and S^{2-}.

Introduction

Transition-metal ions are toxic, causing serious environmental and health issues.[1,2] As one of most common transition-metal ions, Cu^{2+} is one of the highly toxic and global widespread pollutants. As the third most abundant transition metal in the human body, Cu^{2+} plays a vital role in many biological processes.[3–5] Some reports showed that excessive levels of Cu^{2+} accumulated could induce severe neurodegenerative diseases, such as Menkes and Wilson's diseases, familial amyotrophic lateral sclerosis, prion disease and Alzheimer's disease.[6–11] Hence, there remains a significant challenge for development of rapid detection and removal of copper from pollutants. Currently, many techniques have been reported for detecting of Cu^{2+} ion, including atomic absorption spectrometry, inductively coupled plasma atomic emission spectroscopy.[12–16] On the other hand, fluorescent chemosensors have attracted considerable attention due to its simplicity, low-cost and sensitivity. In past few years, many chemosensors with "turn-off" signal upon binding of Cu^{2+} have been reported.[17–19] However, it is not as sensitive as fluorescene enhancement response.[20–26] Therefore, it is also necessary to design and synthesize fluorescent probes of "turn-on" type in aqueous systems, especially for the response enhancement.

Recently, the hydrogen sulfide (H_2S) has proved as a novel gasotransmitter, and exhibited important physiological function like nitric oxide (NO), carbon monoxide (CO) in animal systems.[27,28] The sulfur anion is also an important anion in biological and environmental samples. Most environmental sulfides are released by industries which are involved in conversion of sulfur, such as preparation of sulfuric acid and dyes, cosmetic manufacturing, and production of wood pulp. On the other hand, sulfide anions can also be generated from microbial reduction of sulfate by anaerobic bacteria or from the sulfur-containing amino acids in meat protein.[29] The protonated forms of sulfur, such as HS^- or H_2S are more toxic than sulfide. If mammal drinks the water contaminated with sulfide, it will damage mucous membranes and cause respiratory problem. For example, low concentration of hydrogen sulfide has been proven to produce dizziness, while higher concentration can cause loss of consciousness, permanent damage of brain tissues, or even suffocation.[30,31] However, current major methods for H_2S detection, such as inductively coupled plasma atomic emission spectroscopy and electrochemical determination, titration and ion chromatography, often require complicated sample processing, which would lead to predicament for accurate analysis of this important molecule.[32–36] Therefore, development of a quick and sensitive method for immediate sulfide detection in aqueous media is of high interest.

Recently, rhodamine B-based dyes have been widely used as fluorescence reporting groups due to their excellent spectroscopic properties, such as large molar extinction coefficient, high fluorescence quantum yields, long absorption and emission wavelength.[37] The sensing mechanisms of these chemosensors probes are mainly based on the structure changes of spirocyclic towards its open-cycle forms.[38–45] On the grounds of these strategies, we designed a novel rhodamine B moiety of **L** as a "turn-on" fluorescent probe for Cu^{2+} sensing in aqueous

[a]*College of Chemistry and Chemical Engineering, Lanzhou University, Lanzhou 730000, PR China. E-mail: yansq@lzu.edu.cn; Fax: +86 931 8912582; Tel: +86 931 8912582*

[b]*Huayin Ordnance Test Center, Huayin 714200, China*

† Electronic supplementary information (ESI) available. See DOI: 10.1039/c3ra45931d

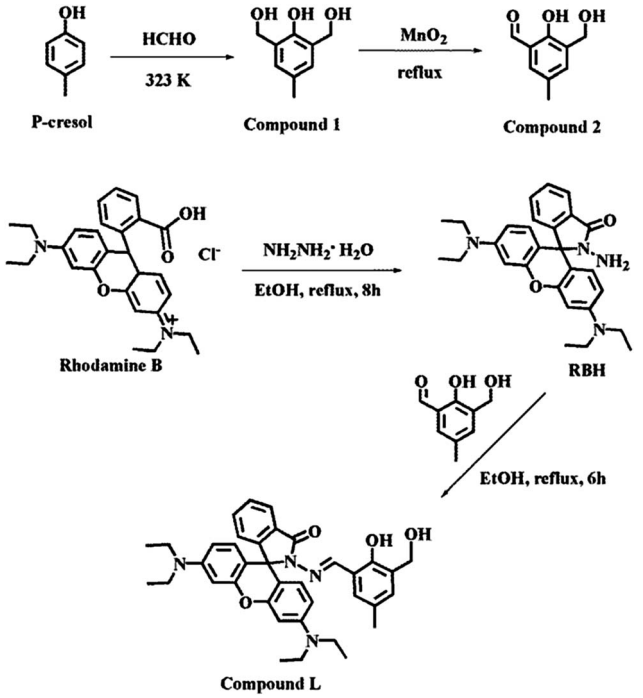

Scheme 1 Synthesis of the fluorescent sensor L.

solution (Scheme 1). In the absent of Cu^{2+} ions, the **L** exists in spirocyclic form, which is colorless with weak fluorescent intensity. Upon addition of Cu^{2+} ion into **L**, the spirocycle structure opened and the solution showed clear pink color, which also generated a fluorescence enhancement response. Additionally, high selectivity toward Cu^{2+} ion over other metal ions was clearly observed. Meanwhile, we also found **L**–Cu^{2+} complex can be employed to detect sulfide. By adding sulfide to the solution of **L**–Cu^{2+} complex, the color of the aqueous change from pink to colorless.

Experimental

Reagents

All reagents and solvents were purchased from commercial suppliers. All chemicals used in this work were of analytical reagent grade and used without further purification. The solutions of the metal ions were prepared from $NaNO_3$, $Mg(NO_3)_2 \cdot 6H_2O$, $Al(NO_3)_3 \cdot 9H_2O$, KNO_3, $Ca(NO_3)_2 \cdot 4H_2O$, $Cr(NO_3)_3 \cdot 9H_2O$, $MnCl_2 \cdot 4H_2O$, $Fe(NO_3)_3 \cdot 9H_2O$, $FeCl_2 \cdot 4H_2O$, $Co(NO_3)_2 \cdot 6H_2O$, $Ni(NO_3)_2 \cdot 6H_2O$, $Cu(NO_3)_2 \cdot 3H_2O$, $Zn(NO_3)_2 \cdot 6H_2O$, $AgNO_3$, $Cd(NO_3)_2 \cdot 4H_2O$, $Ba(NO_3)_2$, $Hg(NO_3)_2 \cdot 0.5H_2O$, $Pb(NO_3)_2$. The solutions of anions were prepared from $NaNO_2$, $NaNO_3$, KCN, KSCN, Na_2SO_4, Na_2SO_3, $Na_3PO_4 \cdot 12H_2O$, Na_2HPO_4, KH_2PO_4, NaAc, NaCl, NaBr, KI, Na_2S. Tris–HCl buffer solutions (1×10^{-2} mol L^{-1}, pH 7.2) and all other solutions were prepared in deionized water.

Instruments

^1H and ^{13}C NMR spectra were taken on a Varian Mercury 300 MHz NMR spectrometer in $CDCl_3$ solutions, with tetramethylsilane (TMS, 0.00 ppm) as an internal standard. Absorption spectra were determined on a Varian UV-Cary100 UV-vis spectrophotometer. Fluorescence spectra measurements were performed on a Hitachi F-4500 fluorescence spectrophotometer. Mass spectra were obtained on a Bruker Daltonics-esquire 6000 mass spectrometer. All pH values were recorded on a PHS-3C digital pH meter (Shanghai, China). All spectra were recorded at room temperature.

Synthesis of compound 2

Compound **2** was synthesized based on the reported procedures with minor changes.[46] The process is the following steps: *p*-cresol (33 g, 0.305 mol) were completely dissolved in sodium hydroxide solution (10 mol L^{-1}, 50 ml). Following full development of a gold color, paraformaldehyde (18 g, 0.6 mol) was added to the solution. The resulting solution was heated to 323 K for 1 hour with a magnetic stirrer bar, and then cooled to room temperature. The yellow solid was collected and dissolved again in hot water. The pH value was adjusted to 3 with HCl (2 mol L^{-1}). The yellow precipitate was collected by filtration and dried overnight in a vacuum oven at 323 K, which afforded a creamy yellow solid compound **1**. Then, compound **1** (10 g, 0.06 mol) was added to 300 ml of $CHCl_3$ in a 500 ml round bottom flask, afterwards, activated MnO_2 (21.7 g, 0.25 mol) was added to the solution with mechanically stirring and refluxing overnight, after which the reaction was cooled to room temperature and filtered, washed with $CHCl_3$ thoroughly until the filtrate became colorless. After the solvent was evaporated under reduced pressure, the crude product was purified by flash column chromatography on silica gel (petroleum ether–ethyl acetate = 2 : 1, v/v), affording compound **2** as yellow solid (6.27 g, yields: 62.89%). ^{1}HNMR ($CDCl_3$, 400 MHz): δ 2.22 (s, 3H, Ar–CH_3), 3. 01 (s, H, CH_2–OH), 4.60 (s, 2H, Ar–CH_2), 7.15, (s, 1H, Ar–H), 7.30 (s, 1H, Ar–H), 9.72 (s, 1H, N=C–H), 11.03 (s, 1H, Ar–OH) ppm. ^{13}C NMR ($CDCl_3$, 100 MHz): δ 20.09, 59.96, 119.86, 128.88, 128.97, 132.38, 136.66, 157.00, 196.59 ppm.

Synthesis of rhodamine sensor (compound L)

RBH was synthesized from rhodamine B according to the literature method.[47]

RBH (0.30 g, 0.66 mmol) was dissolved in 15 ml absolute ethanol. Excess compound **2** (0.16 g, 0.99 mmol) was added to the reaction mixture, then the mixture was stirred and reflux under N_2 atmosphere for 6 hour. Then the solvent was removed under reduced pressure, and the residue was purified by recrystallization with ethanol as yellow solid (0.29 g, yields: 72.7%). ^{1}HNMR (400 MHz, $CDCl_3$): δ 1.19–1.13 (t, J = 7.0 Hz, 12H, NCH_2CH_3), 2.19 (s, 3H, ben–CH_3), 2.75 (s, 1H, ben–CH_2–OH), 3.37–3.29 (q, J = 7.0 Hz, 8H, NCH_2CH_3), 4.62–4.64 (d, J = 5.5 Hz, 2H, ben–CH_2–OH), 6.25–6.52 (m, 6H, xanthene–H), 6.82–6.79 (d, J = 1.1 Hz, 1H, ben–H), 6.98 (s, 1H, ben–H), 7.11–7.19 (m, 1H, Ar–H), 7.47–7.54 (td, J_1 = 6.5, J_2 = 1.2 Hz, 2H, Ar–H), 7.93–8.04 (m, 1H, Ar–H), 8.91 (s, 1H, N=C–H), 11.17 (s, 1H, ben–OH); ^{13}C NMR (101 MHz, $CDCl_3$): δ 12.60, 20.23, 44.38, 62.09, 66.16, 97.99, 105.13, 108.27, 118.00, 123.37, 124.04, 127.86, 128.09, 128.23, 128.53, 129.37, 130.81, 131.24, 133.56, 149.10, 151.30, 151.83, 153.32, 154.46, 164.33. ESI-MS

spectrometry showed a peak with m/z 605.6 $[M + H]^+$, calculate for $C_{37}H_{40}N_4O_4 = 604.74$. Anal. calcd for $C_{37}H_{40}N_4O_4$ (604.74): C 73.42, H 6.61, N 9.26, O 10.71 found: C 73.21, H 6.65, N 9.06, O 11.08%.

Results and discussion

UV-vis spectroscopic studies of L in presence of Cu^{2+}

The spectra responses of chemosensor **L** in the absence or presence of Cu^{2+} in different pH values were evaluated first. As shown in Fig. 1, the absorption of free **L** was very weak between pH 4 and 10. When the pH value was lower than 4, it showed increased absorption. It was attributed to the ring opening of rhodamine occurred at acid conditions (pH < 4) for strong protonation (Scheme S1†). However, the absorbance intensity had significant enhancement after the addition of Cu^{2+} ion between pH 4 and 9. It was due to the formation of ring-opened **L**–Cu^{2+} complex (Scheme 2). Then under basic conditions, the absorbance intensity decreased due to the formation of $Cu(OH)_2$. The data indicated that **L** has good absorption response for Cu^{2+} under physiological pH conditions. Therefore, further UV-vis studies were carried out in CH_3CN/Tris–HCl solution (1 : 1 v/v, pH = 7.2).

The solution of **L** in CH_3CN/Tris–HCl solution (1 : 1 v/v, pH = 7.2) is colorless. As shown in Fig. 2, the absorption spectra of **L** alone (2×10^{-5} mol L^{-1}) exhibited no band in the region beyond 500 nm, which indicated that **L** was of the spirolactam form. The addition of Cu^{2+} into the solution immediately resulted in a strong absorption band centered at 556 nm, with an obvious color change from colorless to pink. A slight increase at 555 nm after the addition of Fe^{2+} was also observed at the same concentration. We infer that Fe^{2+} ion have lower binging affinity to **L** compared with Cu^{2+} in aqueous media. Under the same conditions, no obvious response could be observed upon the addition of other ions. Therefore, **L** can serve as a "naked-eye" indicator for Cu^{2+} ion. Even in the presence of miscellaneous competitive metal ions, the addition of Cu^{2+} ion still resulted in a large absorption change at 556 nm (Fig. 3). This indicates that the selectivity of **L** to Cu^{2+} ion is excellent in the presence of other competitive cations in acetonitrile–water medium.

Titration experiment showed that the absorption spectra of **L** to Cu^{2+} ion also gradually increased at 401 nm and 556 nm, with higher Cu^{2+} concentration (0–10 × 10^{-5} mol L^{-1}) (Fig. 4). The

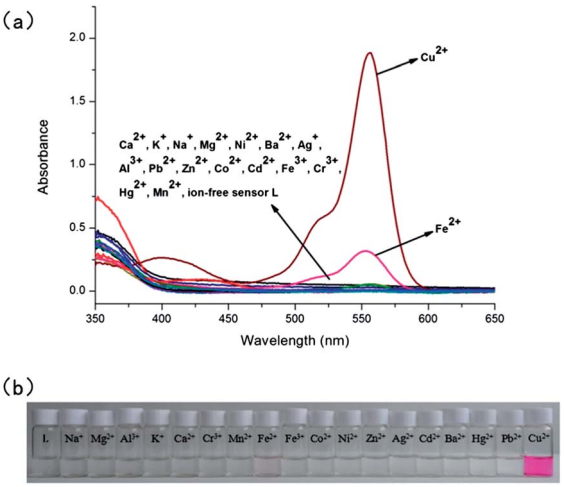

Fig. 2 (a) UV-vis absorption of **L** (2×10^{-5} mol L^{-1}) in the presence of different metal ions (1×10^{-4} mol L^{-1}) in CH_3CN/Tris–HCl solution (1 : 1 v/v, pH = 7.2). (b) Photographs of color changes of 2×10^{-5} mol L^{-1} **L** after the addition of 1×10^{-4} mol L^{-1} various metal ions (from left to right: ion-free sensor **L**, Na^+, Mg^{2+}, Al^{3+}, K^+, Ca^{2+}, Cr^{3+}, Mn^{2+}, Fe^{2+}, Fe^{3+}, Co^{2+}, Ni^{2+}, Zn^{2+}, Ag^{2+}, Cd^{2+}, Ba^{2+}, Hg^{2+}, Pb^{2+}, Cu^{2+}).

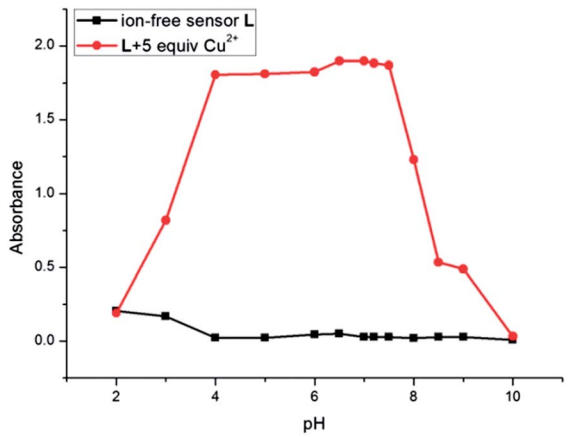

Fig. 1 UV-vis absorption of free **L** (2×10^{-5} mol L^{-1}) and **L** + 5 equiv. of Cu^{2+} ion in CH_3CN/Tris–HCl solution (1 : 1 v/v) with different pH conditions. The absorption wavelength is 556 nm.

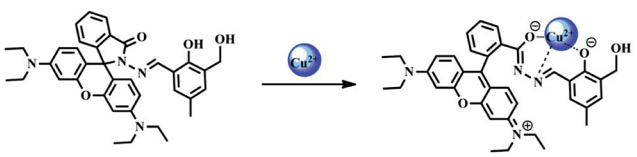

Scheme 2 Proposed binding mode of probe **L** toward Cu^{2+}.

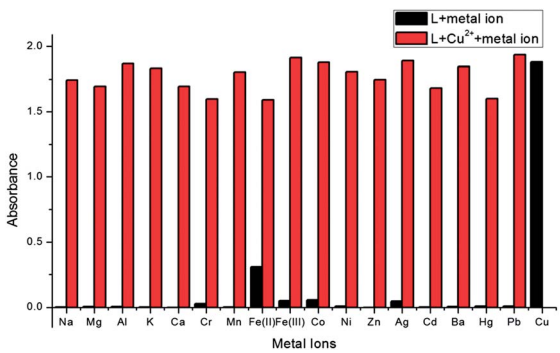

Fig. 3 Absorption spectra of **L** to various metal ions in CH_3CN/Tris–HCl solution (1 : 1 v/v, pH = 7.2). The black bar represent the spectra of **L** (2×10^{-5} mol L^{-1}) obtained with (1×10^{-4} mol L^{-1}) of metal ions. The red bar represents the spectra that occur upon the subsequent addition of (1×10^{-4} mol L^{-1}) of Cu^{2+} to the above mentioned solutions. The absorption wavelength is 556 nm.

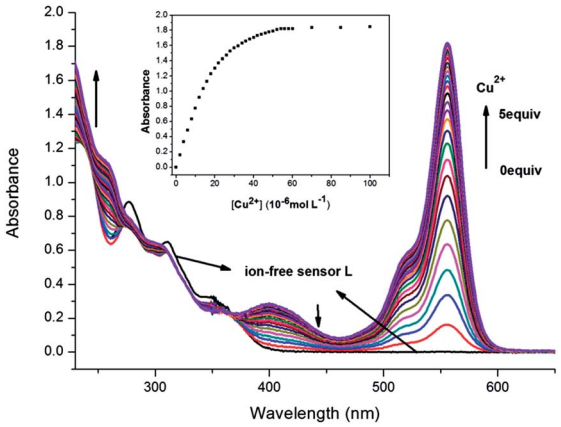

Fig. 4 UV-vis spectra change of L (2×10^{-5} mol L^{-1}) upon the addition of increasing amounts of Cu^{2+} ion in CH_3CN/Tris–HCl solution (1 : 1 v/v, pH = 7.2) (from bottom to top: $[Cu^{2+}] = 0, 2, 4, \ldots, 60, 70, 85, 100 \times 10^{-6}$ mol L^{-1}). Inset: absorbance at 556 nm of L as a function of Cu^{2+} concentration.

absorbance at 556 nm had an approximate 643-fold enhancement. The Job's plot was conducted to determine the binding stoichiometry of the **L**–Cu^{2+} complex, wherein the total concentration of **L** and Cu^{2+} ion is 4×10^{-5} mol L^{-1} and the mole fraction of Cu^{2+} ion is in the range from 0 to 1. As shown in Fig. 5, we can observe that the absorbance went through a maximum peak at a molar fraction of about 0.5, indicating a 1 : 1 binding stoichiometry between Cu^{2+} and **L**. To achieve this stoichiometry, carbonyl O, imino N, and phenol O atoms of **L** are the most likely binding sites for Cu^{2+}. The proposed structure of **L**–Cu^{2+} is illustrated in Scheme 2.

Assuming a 1 : 1 association between **L** and Cu^{2+}, the association constant (K_a) of **L**–Cu^{2+} was determined using the Benesi–Hildebrand equation as follows.[48]

$$\frac{1}{A - A_0} = \frac{1}{K_a(A_{max} - A_0)[Cu^{2+}]} + \frac{1}{A_{max} - A_0} \quad (1)$$

A and A_0 represent the absorbance of **L** solution in the presence and absence of Cu^{2+} ion, and A_{max} is the saturated absorbance of **L** in the presence of excess amount of Cu^{2+}. $[Cu^{2+}]$ is the concentration of Cu^{2+} ion added. Plotting of $1/(A - A_0)$ *versus* $1/[Cu^{2+}]$ showed a linear relationship (Fig. 6), which indicates that **L** bound with Cu^{2+} in a 1 : 1 binding stoichiometry, and the association constant K_a is determined from the slope as 6.47×10^4 M^{-1}. The ESI-mass spectra of **L**–Cu^{2+} also showed a 1 : 1 stoichiometry. The unique peak at $m/z = 666.18$, (calcd = 666.27) corresponding to $[CuL]^+$ was clearly observed when Cu^{2+} was added to **L** (Fig. S6†).

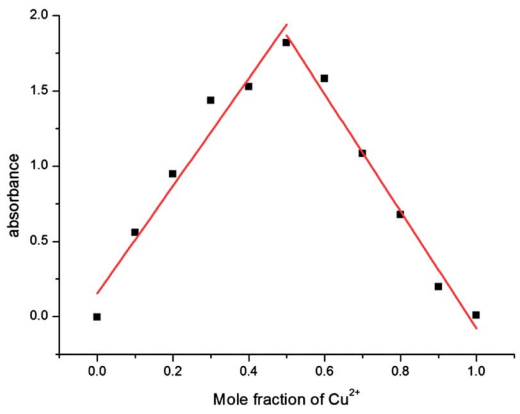

Fig. 5 Job's plot of L and Cu^{2+} in CH_3CN/Tris–HCl solution (1 : 1 v/v, pH = 7.2). The total concentration of L and Cu^{2+} ions is 4×10^{-5} mol L^{-1}. The absorbance was collected at 556 nm.

Fluorescence spectroscopic studies of L in presence of Cu^{2+}

The effects of pH on the sensor **L** was evaluated first. Fig. 7 shows that for ion-free sensor **L**, the fluorescence intensity was strong at pH < 6. It was due to the ring opening of rhodamine for the strong protonation. The fluorescence intensities of ion-free sensor **L** gradually decreased with the increase of pH value.[49] In the pH range from 6 to 10, the fluorescence signal of **L** without Cu^{2+} ion was weak. Upon the addition of Cu^{2+} ion, there was an obvious fluorescence emission at 581 nm in pH from 6 to 9. This result suggested that **L** could act as a fluorescent probe for Cu^{2+}

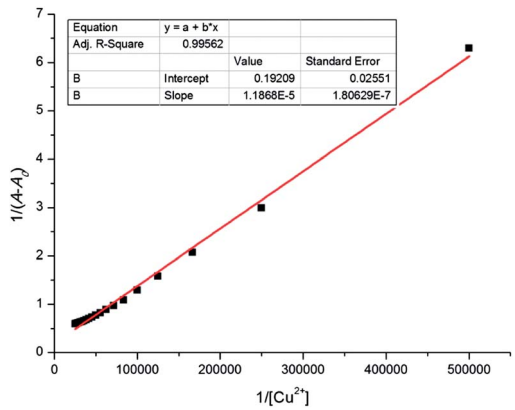

Fig. 6 Benesi–Hildebrand plot (absorbance at 556 nm) of L using eqn (1), assuming 1 : 1 stoichiometry for association between L and Cu^{2+}.

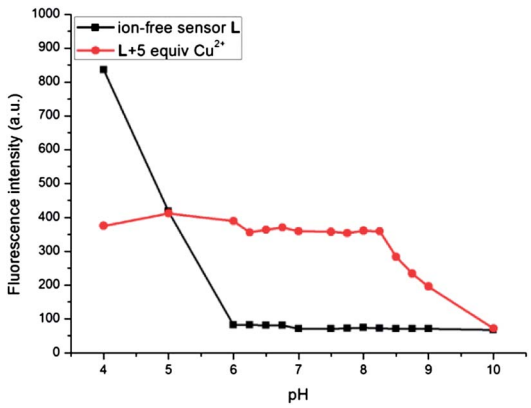

Fig. 7 Fluorescence intensity of free L (2×10^{-5} mol L^{-1}) and L + 5 equiv. of Cu^{2+} ion in CH_3CN/Tris–HCl solution (1 : 1 v/v) with different pH conditions. The excitation wavelength is 530 nm. The emission wavelength is 581 nm.

under physiological conditions (*i.e.* pH 7.2). The experiments have also been conducted in Tris–HCl solutions, wherein the selectivity of sensor **L** towards Cu^{2+} is also good. However, the fluorescence intensity in Tris–HCl solutions is not as strong as that in mixed solvents of acetonitrile and Tris–HCl buffer. Therefore, further fluorescent studies were also carried out in CH_3CN/Tris–HCl solution (1 : 1 v/v, pH = 7.2).

L in CH_3CN/Tris–HCl solution (1 : 1 v/v, pH = 7.2) showed a very weak fluorescence in the absence of metal ions when excited at 530 nm. However, the addition of Cu^{2+} ion resulted in remarkably enhanced fluorescence intensity. Under the same condition, additions of other metal ions including Na^+, Mg^{2+}, Al^{3+}, K^+, Ca^{2+}, Cr^{3+}, Mn^{2+}, Fe^{3+}, Co^{2+}, Ni^{2+}, Zn^{2+}, Ag^+, Cd^{2+}, Ba^{2+}, Hg^{2+} and Pb^{2+} did not cause any discernible changes. On the other hand, the Fe^{2+}–ligand complex, in contrast to the rest of the ions in study, exhibited lower fluorescence intensity than the free ligand (Fig. 8). Similarly, parallel experiments in the presence of potentially competitive metal ions were also carried out (Fig. 9) and the results suggested that the fluorescent recognition of Cu^{2+} by **L** was hardly influenced by other co-existing metal ions.

From the fluorescence titration experiments (Fig. 10), upon addition of Cu^{2+} into CH_3CN/Tris–HCl solution (1 : 1 v/v, pH = 7.2) of **L**, a new emission band centered at 572 nm (the excitation wavelength is 530 nm) was developed. Similar to the absorption response, the fluorescence intensity increased gradually with higher Cu^{2+} concentration. Meanwhile, the emission band underwent a slightly red-shifted from 572 to 581 nm after 2 equiv. of Cu^{2+} were added. The fluorescence intensity at 581 nm had an approximate 7-fold enhancement. The red-shift of the emission peak can be ascribed to the recombination of the orbitals after the formation of ring-opened **L**–Cu^{2+} complex. The emission intensity of ion-free sensor **L** was measured 10 times and the standard deviation of blank measurements was determined. The fluorescence intensity of **L** (2×10^{-5} mol L^{-1}) at 581 nm was found to increase linearly with the concentration of Cu^{2+} in range of 0–0.8 $\times$ 10^{-5} mol L^{-1} (R^2 = 0.9910) (Fig. S7†). The detection limit was then calculated with the eqn (2):[31]

$$\text{Detection limit} = 3\sigma/k \quad (2)$$

where σ is the standard deviation of blank measurement, and k is the slope of the intensity *versus* Cu^{2+} concentration. The detection limit of Cu^{2+} in CH_3CN/Tris–HCl solution (1 : 1 v/v, pH = 7.2) was measured to be 2.43 $\times$ 10^{-8} mol L^{-1}.

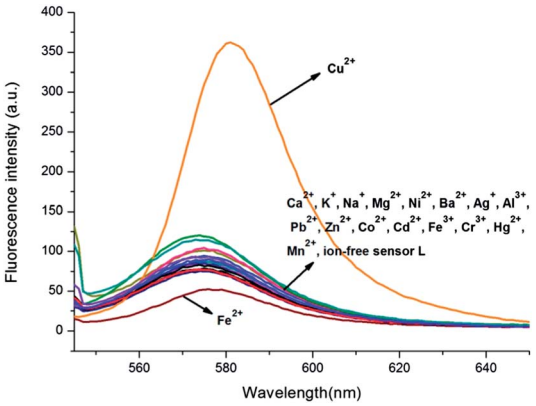

Fig. 8 Fluorescence of **L** (2×10^{-5} mol L^{-1}) in the presence of different metal ions (1×10^{-4} mol L^{-1}) in CH_3CN/Tris–HCl solution (1 : 1 v/v, pH = 7.2). The excitation wavelength is 530 nm.

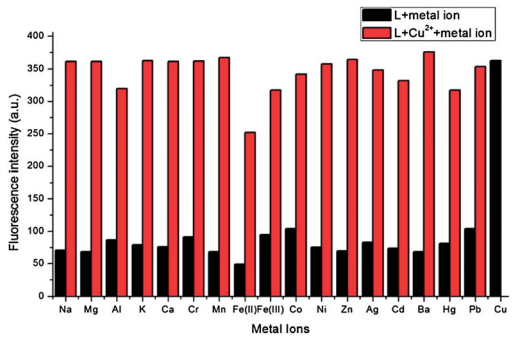

Fig. 9 Fluorescence spectra of **L** to various metal ions in CH_3CN/Tris–HCl solution (1 : 1 v/v, pH = 7.2), the black bar represent the spectra of **L** (2×10^{-5} mol L^{-1}) obtained with (1×10^{-4} mol L^{-1}) of metal ions. The red bar represents the spectra that occur upon the subsequent addition of (1×10^{-4} mol L^{-1}) of Cu^{2+} to the above mentioned solutions. The excitation wavelength is 530 nm. The emission wavelength is 581 nm.

Theoretical calculations

In order to further verify the configuration of **L**–Cu^{2+}, we carried out density functional theory (DFT) calculations with the B3LYP exchange functions using Gaussian 09 package, and introduce the LANL2DZ effective core potential (ECP) to represent the core electrons of the Cu atom. The valence electrons are described by LANL2DZ basis set, while all the other atoms are described commonly by 6-31G(d) basis set. All the thermodynamic data are obtained at this computational level. The molecule forms a

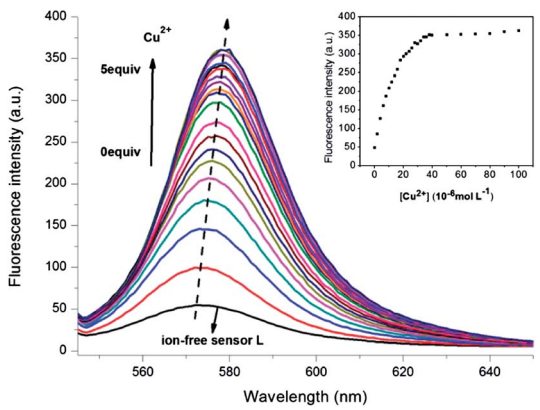

Fig. 10 Fluorescence emission spectra changes of **L** (2×10^{-5} mol L^{-1}) upon the addition of increasing amounts of Cu^{2+} ion in CH_3CN/Tris–HCl solution (1 : 1 v/v, pH = 7.2) (from bottom to top: $[Cu^{2+}]$ = 0, 2, 4, …, 40, 50, 60, 70, 80, 90, 100 $\times$ 10^{-6} mol L^{-1}). Inset: fluorescence titration profile of **L** at 581 nm in increasing of Cu^{2+} concentration.

planar structure, as displayed in Fig. 11. The Cu–N bond length is 1.975 Å, and the distances of Cu–O_1, Cu–O_2, Cu–O_3 are 1.992, 1.912, 1.978 Å, respectively. The optimized configuration shows that Cu^{2+} ions occupy the acylhydrazone coordination centers of **L** at the same time.

UV-vis spectroscopic studies of L–Cu^{2+} complex in presence of S^{2-}

We have further studied the influence of different anions on UV-vis absorbance of **L**–Cu^{2+} complex. Upon addition of Na_2S to **L** (2×10^{-5} mol L^{-1}) and Cu^{2+} (4×10^{-5} mol L^{-1}) complex in CH_3CN/Tris–HCl solution (1 : 1 v/v, pH = 7.2), the UV-vis absorption was decreased and the color of the **L**–Cu^{2+} complex changed from pink to colorless. The optical properties of the **L**–Cu^{2+} complex were also studied in the presence of different anions such as CN^-, SCN^-, SO_3^{2-}, SO_4^{2-}, PO_4^{3-}, HPO_4^{2-}, $H_2PO_4^-$, Cl^-, Br^-, I^-, NO_2^-, NO_3^-, and AcO^-. It is worth noted that only by adding S^{2-} into the solution of **L**–Cu^{2+} could cause this change, whereas other anions failed to produce any discernible spectral change (Fig. 12). For further investigation, a solution of **L** in CH_3CN/Tris–HCl buffer (1 : 1 v/v, pH = 7.2) containing 2 equiv. of Cu^{2+} was titrated by the solution of Na_2S. The UV-vis spectral pattern of the titration experiment was similar but in reverse direction to the titration curve obtained with Cu^{2+} (Fig. 13). Upon the addition of S^{2-} to **L**–Cu^{2+} complex, black precipitate was formed. This phenomenon showed that Cu^{2+} released from complex **L**–Cu^{2+} was captured by sulfide anion to produce CuS. The formation of CuS was also ascertained by the XRD measurement. The sensing capability of **L**–Cu^{2+} complex was further tested in the presence of other anions, which may interfere the estimation of copper and sulfide

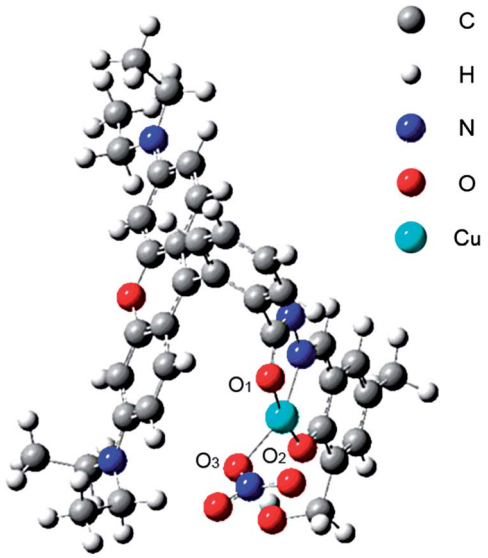

Fig. 11 Calculated energy-minimized structure of **L** with Cu^{2+}.

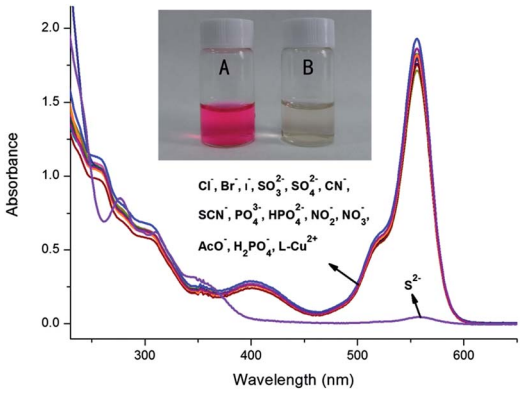

Fig. 12 UV-vis titration spectra of **L** (2×10^{-5} mol L^{-1}) with 4×10^{-5} mol L^{-1} of Cu^{2+} upon addition of different anions (4×10^{-5} mol L^{-1}) in CH_3CN/Tris–HCl solution (1 : 1 v/v, pH = 7.2) (inset, A: **L** + Cu^{2+}. B: **L** + Cu^{2+} + S^{2-}).

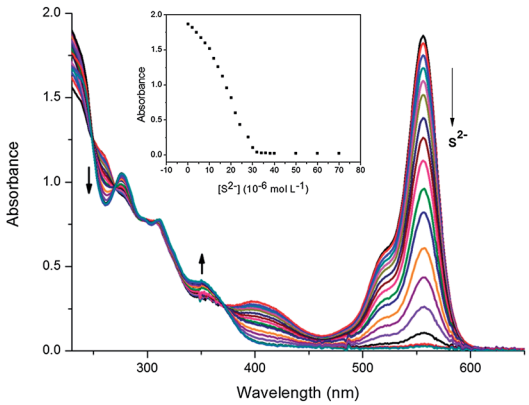

Fig. 13 UV-vis titration spectra of **L** (2×10^{-5} mol L^{-1}) with 4×10^{-5} mol L^{-1} of Cu^{2+} upon addition of sodium sulfide (4×10^{-5} mol L^{-1}) in CH_3CN/Tris–HCl solution (1 : 1 v/v, pH = 7.2) (from top to bottom: $[S^{2-}] = 0, 2, 4, \ldots, 40, 50, 60, 70 \times 10^{-6}$ mol L^{-1}). Inset: changes in the absorbance at 556 nm with incremental addition of S^{2-}.

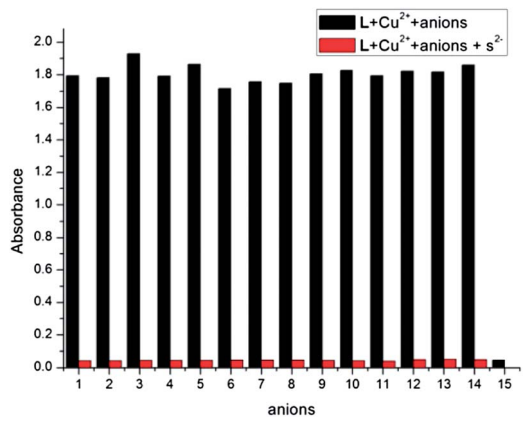

Fig. 14 UV-vis responses of **L**–Cu^{2+} to various anions in CH_3CN/Tris–HCl solution (1 : 1 v/v, pH = 7.2). The black bars represent the absorbance responses of **L** (2×10^{-5} mol L^{-1}) and Cu^{2+} ion (4×10^{-5} mol L^{-1}) in the presence of anions (4×10^{-5} mol L^{-1}) of interest. The red bars represent the change of the absorbance that occurs upon the subsequent addition of S^{2-} (4×10^{-5} mol L^{-1}) to the above solution. The intensities were recorded at 556 nm. (1) **L**–Cu^{2+} (2) CN^- (3) SCN^- (4) SO_3^{2-} (5) SO_4^{2-} (6) PO_4^{3-} (7) HPO_4^{2-} (8) $H_2PO_4^-$ (9) Cl^- (10) Br^- (11) I^- (12) NO_2^- (13) NO_3^- (14) AcO^- (15) S^{2-}.

(Fig. 14). The receptor **L**–Cu^{2+} complex is well selective in detecting sulfur in the presence of other competitive anions. The mass spectrum of the **L**–Cu^{2+} system was also studied in the presence of S^{2-}. ESI-MS of the above media displayed a molecular peak [**L** + H^+] at *m*/*z* 605.6 and a molecular-ion peak [**L** + Na^+] at *m*/*z* 627.5 which confirmed the identity of free **L** (Fig. S8†).

Conclusions

In summary, a rhodamine-based fluorimetric probe **L** was designed and synthesized. Studies showed that **L** exhibited highly selective binding with Cu^{2+} over other metal ions with a fluorescence turn-on effect. The chemosensor **L** displayed a one-to-one complex formation with Cu^{2+} ions in a broad pH range. Obvious increases in colorimetric changes were observed upon the addition of Cu^{2+} into the CH_3CN/Tris–HCl solution (1 : 1 v/v, pH = 7.2) of chemosensor **L**. The complex formed between **L** and Cu^{2+} is dissociable only in the presence of sulfide anion and the color changed from pink to colorless, which makes the **L**–Cu^{2+} complex an efficient sensor for sulfide anions.

Acknowledgements

The authors acknowledge financial support from the NSFC (Grants 21301082), the Natural Science Foundation of Gansu (no. 1308RJYA028) and Huayin Ordnance Test Center. We thank Prof. Renqi Wang for giving many suggestions on this work.

Notes and references

1 Q. Zhao, F. Y. Li and C. H. Huang, *Chem. Soc. Rev.*, 2010, **39**, 3007–3030.
2 D. T. Quang and J. S. Kim, *Chem. Rev.*, 2010, **110**, 6280–6301.
3 S. J. Lippard and J. M. Berg, *Principles of Bioinorganic Chemistry*, University Science Books, Mill Valley, CA, 1994.
4 E. L. Que, D. W. Domaille and C. J. Chang, *Chem. Rev.*, 2008, **108**, 1517–1549.
5 M. C. Linder and M. Hazegh-Azam, *Am. J. Clin. Nutr.*, 1996, **63**, 797S–811S.
6 E. Gaggelli, H. Kozlowski, D. Valensin and G. Valensin, *Chem. Rev.*, 2006, **106**, 1995–2044.
7 D. R. Brown and H. Kozlowski, *Dalton Trans.*, 2004, 1907–1917.
8 G. L. Millhauser, Copper binding in the prion protein, *Acc. Chem. Res.*, 2004, **37**, 79–85.
9 R. Uauy, M. Olivares and M. Gonzalez, *Am. J. Clin. Nutr.*, 1998, **67**, 952S–959S.
10 K. J. Barnham, C. L. Masters and A. I. Bush, *Nat. Rev. Drug Discovery*, 2004, **3**, 205–214.
11 B. E. Kim, T. Nevitt and D. J. Thiele, *Nat. Chem. Biol.*, 2008, **4**, 176–185.
12 J. R. Chen and K. C. Teo, *Anal. Chim. Acta*, 2001, **450**, 215–222.
13 T. W. Lin and S. D. Huang, *Anal. Chem.*, 2001, **73**, 4319–4325.
14 O. Abollino, M. Aceto, M. C. Bruzzoniti, E. Mentasti and C. Sarzanini, *Anal. Chim. Acta*, 1998, **375**, 299–306.
15 A. Vaisanen, R. Suontamo, J. Silvonen and J. Rintala, *Anal. Bioanal. Chem.*, 2002, **373**, 93–97.
16 R. Krämer, *Angew. Chem., Int. Ed.*, 1998, **37**, 772–773.
17 N. Shao, Y. Zhang, S. M. Cheung, R. H. Yang, W. H. Chan, T. Mo, *et al.*, *Anal. Chem.*, 2005, **77**, 7294–7303.
18 S. H. Kim, J. S. Kim, S. M. Park and S. K. Chang, *Org. Lett.*, 2006, **8**, 371–374.
19 Y. Luo, Y. Li, B. Q. Lv, Z. D. Zhou, D. Xiao and M. M. F. Choi, *Microchim. Acta*, 2009, **164**, 411–417.
20 C. W. Yu, J. Zhang, R. Wang and L. X. Chen, *Org. Biomol. Chem.*, 2010, **8**, 5277–5279.
21 J. Zhang, C. W. Yu, S. Y. Qian, G. Lu and J. L. Chen, *Dyes Pigm.*, 2012, **92**, 1370–1375.
22 Z. P. Dong, X. Tian, Y. Z. Chen, J. R. Hou and J. T. Ma, *RSC Adv.*, 2013, **3**, 2227–2233.
23 C. W. Yu, L. X. Chen, J. Zhang, J. H. Li, P. Liu, W. H. Wang, *et al.*, *Talanta*, 2011, **85**, 1627–1633.
24 Z. Q. Hu, X. M. Wang, Y. C. Feng, L. Ding and H. Y. Lu, *Dyes Pigm.*, 2011, **88**, 257–261.
25 H. Zhu, J. L. Fan, J. Lu, M. M. Hu, J. F. Cao, J. Wang, H. L. Li, X. J. Liu and X. J. Peng, *Talanta*, 2012, **93**, 55–61.
26 G. Sivaraman, T. Anand and D. Chellappa, *RSC Adv.*, 2013, **3**, 17029–17033.
27 A. Kawabataa, T. Ishikia, K. Nagasawaa, S. Yoshidab, Y. Maedaa, T. Takahashia, *et al.*, *Pain*, 2007, **132**, 74–81.
28 R. Wang, *Antioxidants and Redox Signaling*, 2003, vol. 5, pp. 493–501.
29 *Hydrogen Sulfide*, World Health Organization, Geneva, 1981, (Environmental Health Criteria, no. 19).
30 P. A. Patnaik, *Comprehensive Guide to the Hazardous Properties of Chemical Substances*, Wiley, New York, 3rd edn, 2007.
31 C. Kar, M. D. Adhikari, A. Ramesh and G. Das, *Inorg. Chem.*, 2013, **52**, 743–752.
32 M. Colon, J. L. Todoli, M. Hidalgo and M. Iglesias, *Anal. Chim. Acta*, 2008, **609**, 160–168.
33 N. S. Lawrence, R. P. Deo and J. Wang, *Anal. Chim. Acta*, 2004, **517**, 131–137.
34 S. Balasubramanian and V. Pugalenthi, *Water Res.*, 2000, **34**, 4201–4206.
35 Z. Pawlak and A. S. Pawlak, *Talanta*, 1999, **48**, 347–353.
36 C. Giuriati, S. Cavalli, A. Gorni, D. Badocco and P. Pastore, *J. Chromatogr. A*, 2004, **1023**, 105–112.
37 Y. Zhao, Y. Sun, X. Lv, Y. L. Liu, M. L. Chen and W. Guo, *Org. Biomol. Chem.*, 2010, **8**, 4143–4147.
38 H. Li, J. Fan, J. Du, K. Guo, S. Sun, X. Liu and X. Peng, *Chem. Commun.*, 2010, **46**, 1079–1081.
39 Z. Q. Hu, X. M. Wang, Y. C. Feng, L. Ding and H. Y. Lu, *Dyes Pigm.*, 2011, **88**, 257–261.
40 W. Y. Liu, H. Y. Li, B. X. Zhao and J. Y. Miao, *Org. Biomol. Chem.*, 2011, **9**, 4802–4805.
41 H. N. Kim, M. H. Lee, H. J. Kim, J. S. Kim and J. Yoon, *Chem. Soc. Rev.*, 2008, **37**, 1465–1472.
42 M. Beija, C. A. M. Afonso and J. M. G. Martinho, *Chem. Soc. Rev.*, 2009, **38**, 2410–2433.
43 G. Sivaraman, V. Sathiyaraja and D. Chellappa, *J. Lumin.*, 2014, **145**, 480–485.

44 G. Sivaraman, T. Anand and D. Chellappa, *Analyst*, 2012, **137**, 5881–5884.
45 G. Sivaraman and D. Chellappa, *J. Mater. Chem. B*, 2013, **1**, 5768–5772.
46 L. Ma, L. P. Lu, M. L. Zhu, Q. M. Wang, Y. Li, *et al.*, *Dalton Trans.*, 2011, **40**, 6532–6540.
47 X. F. Yang, X. Q. Guo and Y. B. Zhao, *Talanta*, 2002, **57**, 883–890.
48 H. A. Benesi and J. H. Hildebrand, *J. Am. Chem. Soc.*, 1949, **71**, 2703–2707.
49 M. Z. Tian, X. J. Peng, J. L. Fan, J. Y. Wang and S. G. Sun, *Dyes Pigm.*, 2012, **95**, 112–115.